

*John D. Keller Jr*

NASA LINDSEY  
NASA LINDSEY  
AMES RESEARCH CENTER  
MOFFETT FIELD, CALIF.  
JUL 31 1967

COPY  
No.       

27P.

N/R

NASA

7 N-05 TM

151428

SOME CONSIDERATIONS OF AIRCRAFT CONFIGURATIONS

SUITABLE FOR LONG-RANGE HYPERSONIC FLIGHT

By A. J. Eggers, Jr.

Ames Research Center  
Moffett Field, Calif., U.S.A.

Presented to Symposium on Hypersonic Flow  
Sponsored by the Colston Research Society

University of Bristol, England  
April 6, 1959

(NASA-TM-108684) SOME  
CONSIDERATIONS OF AIRCRAFT  
CONFIGURATIONS SUITABLE FOR  
LONG-RANGE HYPERSONIC FLIGHT  
(NASA) 27 p

N93-71655

Unclass

Z9/05 0151428

NATIONAL AERONAUTICS and SPACE ADMINISTRATION  
WASHINGTON

ORIGINAL PAGE IS  
OF POOR QUALITY

# SOME CONSIDERATIONS OF AIRCRAFT CONFIGURATIONS

## SUITABLE FOR LONG-RANGE HYPERSONIC FLIGHT

By A. J. Eggers, Jr.\*

National Aeronautics and Space Administration  
Ames Research Center  
Moffett Field, Calif.

### SUMMARY

Motion and heating in long-range hypersonic flight are studied with a view to determine how to increase the payload carrying capabilities of aircraft configurations. Particular attention is devoted to boost-glide flight which exploits the range potential of hypersonic speed. At flight speeds up to 18,000 feet per second, corresponding to ranges up to intercontinental magnitude, over half the weight of an aircraft is supported by aerodynamic lift with the result that an increase in lift-drag ratio makes possible an increase in payload. Methods of increasing lift-drag ratio at these speeds, with particular regard to the arrangement of aircraft components, are therefore explored in some detail. It is concluded from elementary momentum considerations that positioning the body entirely below the wing may be an especially attractive method provided wing and body shape are properly selected. Although this conclusion is contrary to the earlier notions of Sänger and others, according to both theory and experiment configurations of the flat-top type can, in fact, develop lift-drag ratios from 15 to 20 percent higher than those of corresponding flat-bottom or symmetrical types. Maximum lift-drag ratios of flat-top aircraft configurations are attractively high, approaching if not exceeding 6 at Mach numbers up to 10. However, at higher Mach numbers these ratios decrease noticeably, and aerodynamic heating tends to assume major proportions.

At flight speeds in excess of 18,000 feet per second, corresponding to Mach numbers approaching 20 and greater, and ranges approaching semiglobal and greater, over half the weight of an aircraft is supported by centrifugal force. In this case, an increase in lift-drag ratio can be detrimental to the payload carrying capabilities of an aircraft because it serves primarily to increase heating and hence the amount of coolant required to protect the vehicle. The more attractive approach appears, in fact, to be to increase both lift and drag to yield relatively low lift-drag ratios and reduced heating,

---

\*Chief, 10- by 14-Inch Supersonic Wind Tunnel Branch

while maintaining adequate maneuverability in flight. It is demonstrated both theoretically and experimentally that asymmetric flat-top configurations of low fineness ratio and developing lift-drag ratios of the order of 1 may be suitable for these purposes. Long-range flight under these circumstances is perhaps best characterized as being sub-satellite in type.

The general implications of these considerations are that with increasing speed and range the trend of hypersonic configurations will be first to more slender shapes with higher lift-drag ratios, and then at ranges the order of semiglobal and greater and speeds approaching satellite speed to more blunt shapes with higher lift and drag.

### INTRODUCTORY REMARKS

Long range is a natural product of flight at speeds which measure in the many thousands of feet per second. When such flight occurs in the earth's atmosphere we term it hypersonic because the speed is large by comparison to the speed of sound. Hypersonic vehicles were initially attractive, as is so often the case, because of their military possibilities deriving primarily from reduced time of travel. Sänger<sup>1</sup> appreciated these possibilities over a quarter of a century ago and, along with Bredt,<sup>2</sup> made perhaps the first attempt to exploit them in designing a long-range bomber that was rocket boosted to speed and altitude, and returned to earth along essentially a glide trajectory. Now, ironically though understandably enough, the simpler ballistic missile has emerged in the course of events to dominate the military scene of long-range hypersonic vehicles. Nevertheless, the fact remains that Sänger's glider concept is far more suited for manned aircraft because it permits reduced decelerations and increased maneuverability in flight through the atmosphere.

Rocket-boosted glide-type vehicles have, of course, received considerable attention in recent times, both in regard to their motion and heating in hypersonic flight. Allen, Neice, and I<sup>3</sup> of the NASA compared these vehicles with ballistic vehicles and supersonic airplanes, and concluded that the glider may be an especially attractive long-range aircraft for either manned or unmanned applications, provided it is designed with careful consideration of aerodynamic efficiency and aerodynamic heating. It is appropriate to initiate the deliberations of this paper with a brief review of these factors in order that we may better attend to the problem of principal interest to us. This problem is the choice of aircraft configurations that are attractive for long-range hypersonic flight in the sense that a relatively large proportion of their take-off mass is payload. While our considerations will apply primarily to gliders, it will be apparent that much of what we conclude applies equally well to related hypersonic aircraft, including those intended for steady-state or sustained flight.

## MOTION AND HEATING OF HYPERSONIC GLIDERS

The trajectory of the boost-glider is shown schematically in figure 1. In the boost phase of flight relatively little range is achieved while speed and altitude are increased in such a manner that at the end of boost the sum of aerodynamic lift and centrifugal force acting on the glider (due to the curvature of its flight path) just counterbalance its weight. If the entire glide trajectory is followed in accordance with this requirement, then we have Sänger's so-called equilibrium glide in which aerodynamic lift is related to weight and velocity of the vehicle by the equation shown in the figure. We easily deduce from this equation that the majority of the weight of the vehicle is supported by aerodynamic lift at speeds less than about three-fourths satellite speed or 18,000 feet per second, while the majority of the weight is supported by centrifugal force at higher speeds. This fact bears importantly on the motion and heating of gliders which we will now consider.

The variation of maximum speed with range of gliders developing lift-drag ratios from 1 to 6 is shown in figure 2. We note, as expected, that increasing lift-drag ratio reduces the speed required for a given range, by very sizable amounts in fact for ranges the order of one-fourth the circumference of the earth, but by decreasing amounts for longer ranges to the point where the reductions are relatively minor at global range. This loss in effectiveness of lift-drag ratio is directly traceable to the fact that at the higher speeds required for the longer ranges most of the weight of the glider is supported by centrifugal force. Now speed is of fundamental importance to us because of the predominant role it plays in determining the take-off mass required to place a glider in flight. If we assume that a rocket motor developing an effective specific impulse of 300 seconds is employed to boost the glider to speed and altitude, then the ratio of take-off mass to glider mass depends on range as shown in figure 3 for the same lift-drag ratios considered previously. Clearly increased  $L/D$  reduces the ratio of take-off mass to glider mass; however, this reduction, like the reduction in velocity, is largest at ranges less than semiglobal and it is progressively decreased in magnitude with increasing range approaching global.

Let us see now how we may refine this observation to treat payload mass which, rather than glider mass, is the quantity of principal interest to us. There are many factors, of course, which tend to reduce payload mass below total mass of a vehicle, however in hypersonic flight aerodynamic heating overshadows all others in this respect. It is generally agreed that the most promising technique for minimizing the amount of heat which must be absorbed by a hypersonic aircraft of the glider type is to radiate it from the surface at a rate approaching, if not equalling, that of the convection

process.<sup>3</sup> The radiation rate at a given flight velocity is, of course, determined by the convective heating rate and the radiating structure of the vehicle. It follows therefore that if we compare a class of vehicles with identical convective heating rates at identical velocities, and with identical radiating structures in the sense that they radiate away the same fraction of convected heat, then the amount of heat which must be absorbed is the same proportion of the total convective heat per unit area for each vehicle. We have made a comparison on this basis<sup>3</sup> in figure 4 which shows the dependence on range of the ratio of heating per unit area to that for a vehicle with  $L/D = 1$ . All vehicles are assumed to be conical in shape with laminar boundary layers, and the calculations again cover lift-drag ratios from 1 to 6. We see the interesting and most important result that increasing lift-drag ratio may markedly reduce unit area heating and hence heat absorbed at ranges less than one-fourth the earth's circumference, whereas at longer ranges it increases this heating, and markedly so at semiglobal distances and greater. If we recall that heat is simply a converted form of the kinetic energy of the vehicles, then the tendency of increased  $L/D$  to reduce heating is not surprising since it derives primarily from the reduction in velocity required for a given range. This reduction is large, as we discovered earlier, at ranges up to one-fourth the earth's circumference and it does, in fact, tend to dominate the heating problem. At longer ranges the reduction in velocity due to increased  $L/D$  is substantially smaller in magnitude; however, and it does not dominate the heating problem. Indeed the fact that the lower  $L/D$  vehicles fly at higher altitudes in less dense air to achieve a given range is the dominant factor, with the result that they experience substantially less heating. Had we considered net heating rather than heating per unit area in this comparison, the curves for the higher  $L/D$ 's would have been displaced somewhat upward as a result of the increased surface areas of the corresponding vehicles. In addition, of course, questions of transitional and turbulent boundary-layer flows would have to be treated in a detailed study of heating; however, for our purposes the information required is in hand. That is, heating and hence coolant requirements are probably no greater, and may be less with higher  $L/D$  gliders at ranges up to the order of one-fourth the earth's circumference. At longer ranges heating and hence coolant requirements are increased by increasing  $L/D$ , assuming major proportions at semiglobal distances and greater.

Since increased coolant means decreased payload, we are obliged to conclude from these and our previous motion considerations that high  $L/D$  glider configurations have relatively attractive payload capabilities in hypersonic flight covering up to intercontinental distances. However, over longer distances increased  $L/D$  loses much of its effectiveness in increasing glider mass, and payload mass may actually be reduced to accommodate more coolant to protect the vehicle from excessive heating. Accordingly, we are urged to consider first high  $L/D$  and then low  $L/D$  configurations in our study of aircraft suitable for hypersonic flight over increasingly long range.

## CONFIGURATIONS DEVELOPING HIGH LIFT-DRAG RATIOS

We can anticipate that an aircraft developing high lift-drag ratios will be slender, and that it will develop these ratios at small angles of attack. The body should, of course, have low pressure drag and be shaped, insofar as possible, to stabilize the vehicle in flight. These factors combine to draw our attention to bodies which are continuously enlarging with distance aft of the nose. They have the virtue of low drag at hypersonic speeds<sup>4</sup> along with the flare effect which contributes to stability.<sup>5</sup> For simplicity then let us consider such a body of revolution mounted symmetrically on a thin wing at zero angle of attack. A front view of this arrangement, along with the disturbance velocities created by the body, is shown at the top of figure 5. Quite obviously the upward momentum generated by pressure forces on the top of the body just cancels the downward momentum generated by pressure forces on the bottom of the body. If we adopt the principle that in order to achieve high  $L/D$  the components of an aircraft should be individually and collectively arranged to impart the maximum downward and the minimum forward momentum to the surrounding air, then the upper half of the body should be eliminated to obtain the arrangement shown in the upper right of the figure. The wing now serves the important function of preserving the downward momentum of the air disturbed by the lower half of the body. Let us consider next the plan view of this configuration shown on the lower left of the figure. The wing extends arbitrarily far beyond the body shock in this view. Now the body can impart downward momentum to the air in the region between its surface and its shock wave. The wing therefore should extend out at least as far as the shock wave in order to preserve this momentum. However, any portion of the wing which extends beyond the shock of the body cannot serve to increase the downward momentum of the air and it will contribute to the forward momentum imparted to the air through the action of friction forces. Thus, the elementary momentum principle suggests that the wing leading edge should coincide with the shock wave created by the body. It can similarly be reasoned that the wing should extend downstream toward, but not beyond, the line along which the body ceases to impart downward momentum to the fluid. Accordingly, it is indicated that the wing trailing edge should, like the leading edge, be swept back and it should join with the body at its base. We are led to suspect then that the configuration should appear in plan view something like the one shown on the lower right of the figure. This shape satisfies the condition of high leading-edge sweep to minimize heating in this region<sup>6</sup> and, too, the resulting wing tends to be of low aspect ratio which is favorable to minimizing structural weight.

Something more may be learned, however, by again viewing the configuration from the front. Such a view is shown in the upper left of figure 6. It is observed that the body imparts lateral as well as downward momentum to the surrounding air. Now according to the

momentum principle, this lateral momentum should be converted into downward momentum and one way in which this may be accomplished without significantly increasing forward momentum is to deflect the wing tips downward about hinge lines in the stream direction as shown in the upper right of the figure. In this location the drooped tips can serve two functions. One of course is to increase lift. Also, and perhaps more important, they are suitably located to provide directional stability and control for the configuration. We have then the crude semblance of a complete aircraft configuration, and this point is demonstrated in the schematic diagram of the vehicle shown at the bottom of the figure. The aircraft is of the flat-top or high-wing type with a laterally symmetric fuselage.<sup>7</sup> Both wing and body contribute substantially to lift. Superficial examination suggests that the wing and body are suitably arranged to obtain stability in pitch, while control in pitch may be derived from wing trailing-edge flaps. The wing should, of course, contribute to damping in roll, while roll control may be obtained by differential operation of wing flaps as ailerons. Finally, directional stability may be derived from the body and the drooped portion of the wing, and directional control may be derived from the tip flaps.

The most important question is, of course, do configurations of this type actually develop high lift-drag ratios at hypersonic speeds. In order to answer this question it is necessary to examine more closely the aerodynamic characteristics of such vehicles. Assuming a linear dependence of lift and interference drag on angle of attack we can estimate maximum lift-drag ratios with the aid of the equations shown in figure 7.\* The familiar equation for maximum  $L/D$  of a symmetrical configuration is shown for reference at the top of the figure. By comparison of this equation with the second equation which holds for the flat-top configuration, it is clear that interference lift at zero angle of attack,  $C_{L_0}$ , definitely tends to increase maximum lift-drag ratio although, as was first pointed out by Migotsky and Adams,<sup>8</sup> this tendency may be somewhat offset by the rate of increase in axial force on the fuselage with angle of attack,  $CA_{\alpha_0}$ . We see as expected from the third equation in the figure that interference lift at zero angle of attack tends to reduce the maximum lift-drag ratio of flat-bottom configurations. Now these conclusions reached by Syvertson and me are quite consistent with those reached about the same time by Ferri<sup>9</sup> and Rossow<sup>10</sup> in their studies of interference effects, and our conceptual thinking conforms in important respects with the deductions of R. T. Jones<sup>11</sup> on general requirements for obtaining high lift-drag ratios in supersonic flight. We have rather particular configurations in mind here, however, and we shall proceed now to study them in some detail.

Maximum lift-drag ratios of flat-top conical configurations have been calculated for high Mach numbers in the manner we have just described. In the calculations base drag was neglected and a 5° half-cone body was used. The results of these calculations are

\* The complete square root term in the denominator of the equations for the asymmetrical configurations is  $2\sqrt{C_{L_\alpha} C_{D_0} - C_{L_0} C_{A_\alpha}}$ . However, for the slender configurations of interest to us  $\left| \begin{matrix} C_{L_0} & C_{A_\alpha} \\ C_{L_\alpha} & C_{D_0} \end{matrix} \right|$  is usually small by comparison to  $\left| \begin{matrix} C_{L_\alpha} & C_{D_0} \end{matrix} \right|$  and can be neglected as we have done.

ORIGINAL PAGE IS  
OF POOR QUALITY

presented in figure 8 for the case of a flat-plate wing with straight leading edges coinciding with the body shock at zero angle of attack. The wing trailing edges were formed by straight lines swept back from the body base and intersecting the leading edges 1.4 body lengths aft of the vertex. It is noted that the plan form changes with the design Mach number. It is not surprising to see that with increasing Mach number and skin friction there is a reduction in maximum lift-drag ratio. However, if skin-friction coefficients are less than 0.006 then the flat-top configurations should be able to develop maximum lift-drag ratios of the order of 6, if not greater, at Mach numbers up to 10. It is interesting to note, too, that the flat-top configurations are consistently capable of achieving higher lift-drag ratios than corresponding flat-bottom configurations, and this advantage increases substantially with decreasing friction drag. The estimated effect of cone angle on maximum lift-drag ratio is shown in figure 9. It is observed that  $L/D$  continuously decreases with increasing cone angle for all friction coefficients. However, it is interesting to note that the  $L/D$  of the configuration with the  $5^\circ$  half-cone body is only slightly less than that for a wing alone. Measured maximum lift-drag ratios for this type of configuration are shown in figure 10 for Mach numbers from 3 to 6. These data were obtained in the 10- by 14-inch wind tunnel of the Ames Research Center, and the test Reynolds numbers measured in the several millions at all but the highest Mach number, where the Reynolds number based on body length was just a little over 1 million. In addition to data for the flat-top configuration, there are also included data for symmetrical and flat-bottom configurations having the same wing, the same length of conical body, and the same body volume. It is observed that the flat-top configuration has the highest lift-drag ratios over the Mach number range, and at the design Mach number of 5 this ratio is only slightly less than 7, exceeding by more than 15 percent the  $L/D$  for the flat-bottom configuration, and by more than 20 percent the  $L/D$  for the more conventional symmetrical configuration. Note too that at the design Mach number theory and experiment are in essential agreement.\*

The effect of wing-tip droop on maximum lift-drag ratios of flat-top configurations is shown in figure 11 for a Mach number of 5. According to the data, increasing the droop angle slightly decreases  $L/D$  for the more slender configuration with the sharp tips, whereas with the blunter configuration having tips cut off normal to the flight direction increasing the droop angle at first increases  $L/D$  and then decreases  $L/D$ . The difference in effect of droop angle observed here is due to the fact that the more slender configuration generates weaker pressures in the regions of the drooped tips, and the area of these tips is smaller. Some additional understanding of these results can be obtained by studying the lift and drag of this basic flat-top configuration. Experimental data on these quantities are presented in figure 12 for a Mach number of 5 and droop angles of  $0^\circ$  and  $60^\circ$ . It is observed that our assumptions of linear lift curves and increased lift due to tip droop near zero angle of attack

---

\*The fact that  $L/D$  for the symmetrical configuration is slightly less than that for the flat bottom configuration is due to the higher surface area of the symmetrical configuration, and to the relatively high proportion of total drag that was friction drag in the tests.



are confirmed by experiment. On the other hand, drooping the tips reduces lift-curve slope, and tends to increase drag at angle of attack with the result that  $(L/D)_{\max}$  is somewhat reduced. Reducing friction drag so that  $(L/D)_{\max}$  occurs at smaller angles of attack will tend to eliminate the reduction in  $L/D$  due to tip droop. This reduction is rather small in any event, however, and may be quite acceptable if the tips are employed to provide directional stability and control.

Thus far in our considerations, we have restricted attention to Mach numbers of the order of 10 and less because of limitations in our theoretical and experimental techniques. A useful tool for extending these considerations to higher Mach numbers is the hypersonic similarity rule of Tsien<sup>12</sup> and Hayes.<sup>13</sup> This rule is summarized for our purposes in figure 13, and it states, in essence, that affinely related slender configurations characterized by the same products of Mach number and thickness to chord ratio, Mach number and span to chord ratio, and Mach number and angle of attack will also be characterized by the same products of Mach number squared and lift coefficient, Mach number cubed and pressure drag coefficient, and Mach number squared and pitching-moment coefficient. Using this rule and the experimental data we discussed earlier, we can, by correcting friction drag to equilibrium flight conditions of vehicles having 20 pounds per square foot wing loading and a fuselage 50 feet in length, estimate maximum lift-drag ratios in flight over a wide range of Mach number. The results of these estimates are presented in figure 14. In these estimates a transition Reynolds number of  $3 \times 10^6$  and base pressure coefficients on the vehicles equal to 70 percent of the vacuum value were assumed. The resulting base drag is the principal cause of reduced lift-drag ratios at Mach numbers below about 7. At Mach numbers in the range from 7 to 10 highest lift-drag ratios are achieved and they are of the order of 6 for the flat-top configurations. With increasing Mach number above 10 there is a steady decline of maximum lift-drag ratio down to a value of more like 4 at a Mach number of 20. This decline occurs in spite of the increased slenderness of the vehicles and it is due to the combined effects of decrease in lift curve slope and increase in the proportion of total drag which is friction drag at the higher flight Mach numbers. Accordingly, while flat-top configurations tend to retain their advantage in lifting efficiency at Mach numbers approaching 20, this advantage is small, it applies to reduced values of  $L/D$ , and it tends to be achieved with configurations which may be impractically slender. At this point, however, we recall from our initial considerations of long-range hypersonic flight that increased lift-drag ratio may actually subtract from over-all flight efficiency at the longer ranges achieved with speeds of the order of 20 times the speed of sound and greater. We concluded, in fact, that low  $L/D$  vehicles may be more attractive for these applications and this is the possibility which we shall now explore in some detail.

## CONFIGURATIONS DEVELOPING LOW LIFT-DRAG RATIOS

It is instructive to initiate this study by taking a rather careful look at the motion and heating of gliders near satellite speed, and we shall identify such vehicles as sub-satellites. Range and heating per unit area of sub-satellites<sup>3,14</sup> are shown in figure 15. The results shown on the left of the figure are for a maximum glide speed equal to 0.9 satellite speed and the independent variable is  $L/D$ . The results shown on the right are for an  $L/D$  of 1 and the independent variable is maximum glide speed. Considering first the range, we note that increasing  $L/D$  from 1 to 3 at 0.9 satellite speed will not even provide semiglobal range, whereas increasing the speed by slightly less than 10 percent to near satellite value will easily provide semiglobal range, or more. Of further importance is the fact that the heating penalty associated with this speed increase is far less than that associated with the increased  $L/D$ . We have further evidence then that increased  $L/D$  is not the way to achieve ranges of the order of semiglobal and greater, but rather the key variable at these distances is speed itself.

Lift-drag ratio is important for other reasons, however, related to decelerations and lateral maneuverability during flight. If we assume a maximum speed approaching satellite speed, these quantities are estimated<sup>14</sup> to vary with  $L/D$  as shown in figure 16. Maximum decelerations seem to be quite high near zero  $L/D$ ; however, for values of  $L/D$  of the order of 1 and greater, these decelerations approximate those of conventional flight. Now maximum lateral range in an equilibrium glide is achieved with about  $45^\circ$  bank angle on a vehicle.<sup>14</sup> Since a vehicle can bank in either of two directions, twice this range is the measure of maximum lateral maneuverability. We see in figure 16 that this maneuverability increases rather rapidly with  $L/D$ , indeed about like the square at the lower  $L/D$ 's. With an  $L/D$  of the order of 1, maximum lateral maneuverability approximates the orbit shift distance per revolution of a low-altitude satellite about the earth, that is about 1500 miles, and this should be ample maneuverability for many sub-satellite applications. The effect on motion and heating of banking to maneuver laterally is shown in figure 17. As we would expect, deceleration and heating rates are increased by banking, while longitudinal range and total heat transfer are decreased.<sup>14</sup> For bank angles up to that for maximum lateral range, however, none of these changes are disconcertingly large being at most the order of 40 percent. From these considerations we conclude, therefore, that sub-satellite vehicles developing lift-drag ratios of the order of 1 may be characterized by adequately low decelerations and adequately high lateral maneuverability for aircraft in the sense that we are discussing them here, and moreover lateral maneuvers need not excessively alter either decelerations or heating.

Having defined the sort of characteristic we might expect of sub-satellites, it is appropriate now to inquire how we might design them to achieve these expectations. Consistent with the  $L/D$  requirements, it

is essential, of course, to reduce the heating problem. Now we know from ballistic missile studies<sup>15</sup> that high-drag shapes have reduced total heating, whereas from airplane studies<sup>3</sup> we know that high-lift shapes have reduced heating rates. We are attracted, therefore, to high-lift, high-drag configurations for sub-satellite applications, and one technique for obtaining such configurations is shown in figure 18. This is by now a familiar technique to us because it consists of obtaining lift by removing the upper half of a body of revolution. In this case, however, we start out with a blunt rather than a slender shape as before, and the resulting flat-top body produces high lift and high drag, rather than high lift-drag ratios as before. Lift may, of course, be achieved by flying symmetrical configurations at angle of attack; however, high-drag bodies of revolution tend to have poor lifting characteristics.\* We will confine our attention therefore to blunt flat-top configurations of the type shown here with a view to assessing their aerodynamic characteristics.\*\*

If we employ Newton's<sup>17</sup> impact theory to estimate the lift and drag of half-cones we obtain the results shown in figure 19. It is indicated that drag coefficient increases continuously with increasing cone angle while lift coefficient reaches a maximum at a cone angle of  $45^\circ$ .\*\*\* As a result, lift-drag ratio decreases continuously with increasing cone angle from a value near 2 at  $20^\circ$  to 0 at  $90^\circ$ . The estimated generalized heating<sup>14</sup> of half-cones initiating their glide at satellite speed is presented in figure 20 as a function of  $L/D$ . The quantities  $H_s$ , heat transfer per unit area to the stagnation region, and  $H_a$ , average heat transfer per unit area, are shown on the left while the corresponding radiation equilibrium temperatures are shown on the right of the figure. The bar over the drag parameter ( $C_D A/m$ ) indicates it has been normalized by dividing through with unit value of the parameter in cubic feet per slug. The quantity  $r_n$  is the nose radius of the vehicle for stagnation heat transfer and the base radius for average heat transfer, the mass is  $m$ , and the surface emissivity is  $\epsilon$ . If we assume nominal values of the drag parameters of the order of unity, then we can interpret heating directly in terms of  $\text{Btu/ft}^2$ , and we can interpret equilibrium temperature directly in terms of  $^\circ\text{R}$ . In this event we see that heating per unit area increases markedly with increasing  $L/D$ , approaching values like  $80,000 \text{ Btu/ft}^2$  in the stagnation region and  $40,000 \text{ Btu/ft}^2$  on an average surface element at an  $L/D$  of 2. We are forcefully reminded therefore that  $L/D$  should be no higher than that required by considerations of decelerations and maneuverability. Now equilibrium surface temperatures are observed to decrease somewhat with increasing  $L/D$ , being generally in the range of  $3000^\circ\text{R}$  or a little less. Clearly these temperatures are within the range of useful strengths of ceramic, if not high-temperature structural materials, and radiation cooling should be achievable to a high degree in practice. In view of the magnitude of the heating, radiation cooling may have to be achieved to a high degree. For

---

\* For example, the initial lift curve slope of right-circular cones approaches zero as the semi-apex angle approaches  $45^\circ$ ,<sup>16</sup> and this slope becomes negative at larger semi-apex angles, tending to promote dynamic instability.

\*\* It is not to be implied that these configurations are thought to be optimum for sub-satellite applications. Indeed, all other things being the same, a flat-bottom body, for example, tends to have less "hot" lifting surface and hence less total heating than the corresponding flat-top body. Accordingly, it is only intended to show here that flat-top configurations may provide a useful compromise in terms of heating, force and moment characteristics.

\*\*\* Base area is the reference area for these coefficients.

ORIGINAL PAGE IS  
OF POOR QUALITY

example, even a small percentage of the heat load may amount to several thousand Btu/ft<sup>2</sup> of surface area of the vehicle, and so the coolant required to absorb this heat can easily add several pounds per square foot to the unit weight of an already relatively heavy structure.

Now it can easily be demonstrated that, irrespective of shape, vehicles developing the same L/D and heating rates will experience the same total heating per unit area if their glide commences at the same velocity. If they are all equipped with the same type radiating structure and have the same weight and heated surface area, then they tend to be equal from the over-all motion and heating point of view, and they tend to have comparable payload carrying capabilities. In this event their relative merit may be determined by their suitability for carrying the payload, that is their flyability.

One method of converting a half-cone body to something resembling a flyable sub-satellite is presented in figure 21. A small wing is located on the top of the body as shown, and the portion of the wing extending aft of the base is hinged to provide elevons for pitch and roll control. Static stability of the configuration is derived primarily from the body, while damping in roll comes mainly from the wing. Generous nose bluntness and filleting at the wing-body junction are provided to minimize heating problems in these regions. Longitudinal force and moment characteristics of a configuration like this have been measured at Mach numbers from about 3 to 13 and are shown in figure 22. Experiment is compared with the predictions of Newtonian theory modified slightly to account for interference effects between the wing and the body. The agreement between theory and experiment is observed to be good on the whole, and the changes in force and moment characteristics with increasing Mach number above 3 are small. Inasmuch as the configuration is relatively blunt over-all, this result is not surprising since it is, in fact, in agreement with the flow-field freeze principle of Oswatitsch.<sup>19</sup> It is also noteworthy that aerodynamic characteristics of the configuration behave in a normal fashion with small changes in angle of attack from zero. Thus, for example, lift-curve slope is positive though small with a value of about 0.02 per deg., and  $C_{m\alpha}$  (moments are taken about the center of volume of the configuration) is essentially constant at the negative value for  $\alpha = 0$ . We have some assurance then that high-lift, high-drag configurations of the flat-top type developing lift-drag ratios of the order of 1 may be designed with suitable flying qualities at supersonic and hypersonic speeds. If the configurations are blunt to the degree of the one just considered, it seems unlikely that they will be capable of a conventional landing, and parachute recovery in the terminal phase of flight will probably be required. If a conventional landing capability is important then basically more slender configurations which can develop higher lift-drag ratios at low speeds may be necessary. It is essential, of course, to minimize hypersonic heating of such configurations insofar as possible, and this may be achieved by flying the vehicle in the manner shown in figure 23. In the sub-satellite portion of flight

the vehicle flies at a high angle of attack giving it "apparent" asymmetric bluntness to provide high lift and high drag. As speed is decreased and the trajectory steepens the angle of attack of the vehicle is reduced to a value giving high lift-drag ratio. The sinking speed is thereby reduced to permit a conventional landing which is on water in the example shown in figure 23.

#### CONCLUDING REMARKS

In conclusion it seems appropriate to summarize our findings on the trends of hypersonic aircraft configurations with increasing speed and range. These trends are shown schematically in figure 24. If we restrict ourselves to glider-type aircraft we can identify a speed-range corridor which is the shaded area in the figure. The boundaries of this corridor are largely determined by the requirement for reasonable payload carrying capabilities of the vehicles. Flight above the upper boundary tends to markedly decrease payload because lift-drag ratios are so low as to require excessively high take-off mass for a given glider mass. Flight below the lower boundary tends to markedly decrease payload at longer ranges because lift-drag ratios are so high as to cause excessive aerodynamic heating, with the result that substantial coolant must be provided to protect the vehicle. Flight below the lower boundary at shorter ranges is unattainable with known techniques for obtaining high lift-drag ratios. The configurations that tend to fly within these boundaries are shown schematically in the shaded area. At first they increase in slenderness with increasing speed and range in order to maintain high lift-drag ratios. At ranges in excess of about one-quarter of the earth's circumference and speeds in excess of about 0.7 satellite speed or 18,000 feet per second, aerodynamic heating becomes the dominant factor with the result that configurations tend to become blunter again in order to minimize this heating. We considered the problems of obtaining high lift-drag ratios at speeds up to about 18,000 feet per second and concluded that configurations with the body situated entirely beneath the wing may develop especially high  $L/D$ 's and may be evolved into something resembling a complete aircraft configuration by drooping the wing tips. Such a configuration is slender in appearance and has essentially a flat top like the example shown in figure 24. Blunter configurations for higher speed, longer range flight may also have a flat top to provide high lift to decrease heating rates along with high drag to reduce total heating. Such a configuration might appear something like the one shown on the right of figure 24. If a conventional landing capability is required of sub-satellites, then they will tend to be basically more slender, with the combination of high lift and high drag being obtained with a high angle of attack to give them "apparent" asymmetric bluntness in hypersonic flight.

## REFERENCES

1. Sanger, Eugen: Raketen-flugtechnik. R. Oldenbourg (Berlin), 1933.
2. Sanger, Eugen, and Bredt, I.: A Rocket Drive for Long Range Bombers. Tech. Information Branch, Navy Department, Trans. CGD-32, 1947.
3. Eggers, Alfred J., Jr., Allen, H. Julian, and Neice, Stanford E.: A Comparative Analysis of the Performance of Long-Range Hypervelocity Vehicles. NACA RM A54L10, 1955. (Now NACA TN 4046)
4. Eggers, A. J., Jr., Resnikoff, Meyer M., and Dennis, David H.: Bodies of Revolution Having Minimum Drag at High Supersonic Airspeeds. NACA RM A51K27, 1952. (Now NACA Rep. 1306)
5. Eggers, A. J., Jr., and Syvertson, Clarence A.: Experimental Investigation of a Body Flare for Obtaining Pitch Stability and a Body Flap for Obtaining Pitch Control in Hypersonic Flight. NACA RM A54J13, 1954.
6. Eggers, A. J., Jr., Hansen, C. Frederick, and Cunningham, Bernard E.: Stagnation-Point Heat Transfer to Blunt Shapes in Hypersonic Flight, Including Effects of Yaw. NACA RM A55E02, 1955. (Now NACA TN 4229)
7. Eggers, A. J., Jr., and Syvertson, Clarence A.: Aircraft Configurations Developing High Lift-Drag Ratios at High Supersonic Speeds. NACA RM A55L05, 1956.
8. Migotsky, Eugene, and Adams, Gaynor J.: Some Properties of Wing and Half-Body Arrangements at Supersonic Speeds. NACA RM A57E15, 1957.
9. Ferri, Antonio, Clarke, Joseph H., and Casaccio, Anthony: Drag Reduction in Lifting Systems by Advantageous Use of Interference. PIBAL Rep. 272, Polytechnic Institute of Brooklyn, Dept. of Aeronautical Engineering and Applied Mechanics, May 1955.
10. Rossow, Vernon J.: A Theoretical Study of the Lifting Efficiency at Supersonic Speeds of Wings Utilizing Indirect Lift Induced by Vertical Surfaces. NACA RM A55L08, 1956.
11. Jones, Robert T.: Minimum Wave Drag for Arbitrary Arrangements of Wings and Bodies. NACA Rep. 1335, 1957. (Supersedes NACA TN 3530)

12. Tsien, Hsue-shen: Similarity Laws of Hypersonic Flows. Jour. Math. and Phys., vol. 25, no. 3, Oct. 1946, pp. 247-251.
13. Hayes, Wallace D.: On Hypersonic Similitude. Quart. Appl. Math., vol. V, no. 1, Apr. 1947, pp. 105-106.
14. Eggers, A. J., Jr.: The Possibility of a Safe Landing. Space Technology, ch. 13. John Wiley and Sons, Inc., 1959.
15. Allen, H. Julian, and Eggers, A. J., Jr.: A Study of the Motion and Aerodynamic Heating of Missiles Entering the Earth's Atmosphere at High Supersonic Speeds. NACA TN 4047, 1957.
16. Ames Research Staff: Equations, Tables, and Charts for Compressible Flow. NACA Rep. 1135, 1953.
17. Newton, Isaac: Principia - Motte's Translation Revised. Univ. of Calif. Press, 1946, pp. 333, 657-661.
18. Batdorf, Samuel B.: Structural Problems in Hypersonic Flight. Jet Propulsion, vol. 27, no. 11, Nov. 1957, pp. 1157-1161.
19. Oswatitsch, Klaus: Similarity Laws for Hypersonic Flow. KTH Aero. TN 16, Royal Inst. of Tech., Division of Aeronautics, Stockholm, Sweden, 1950.

# BOOST-GLIDE FLIGHT

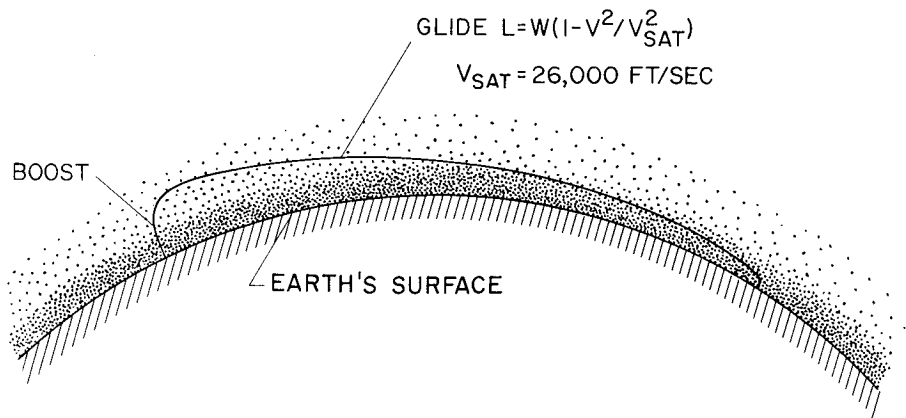


Figure 1.

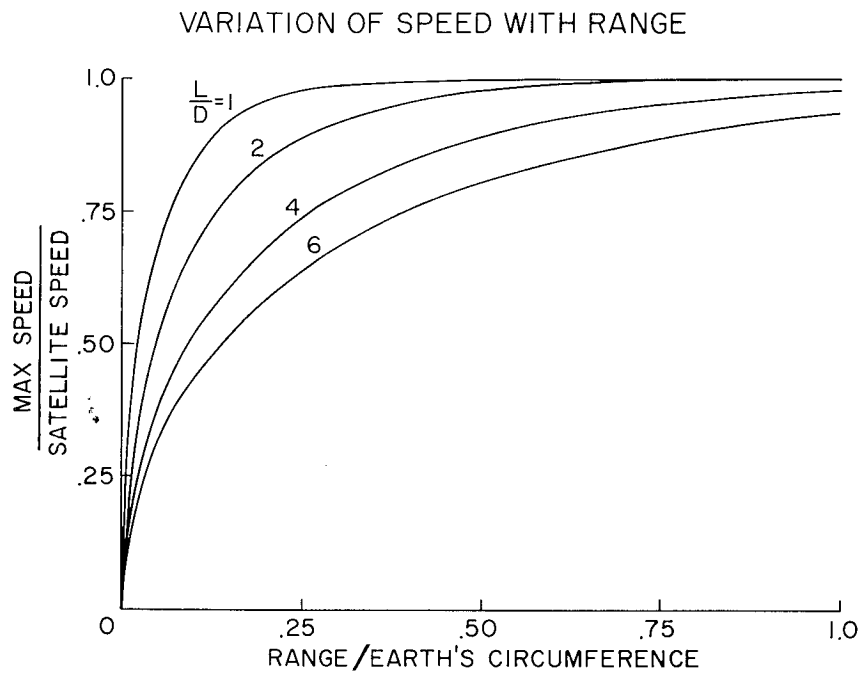


Figure 2.



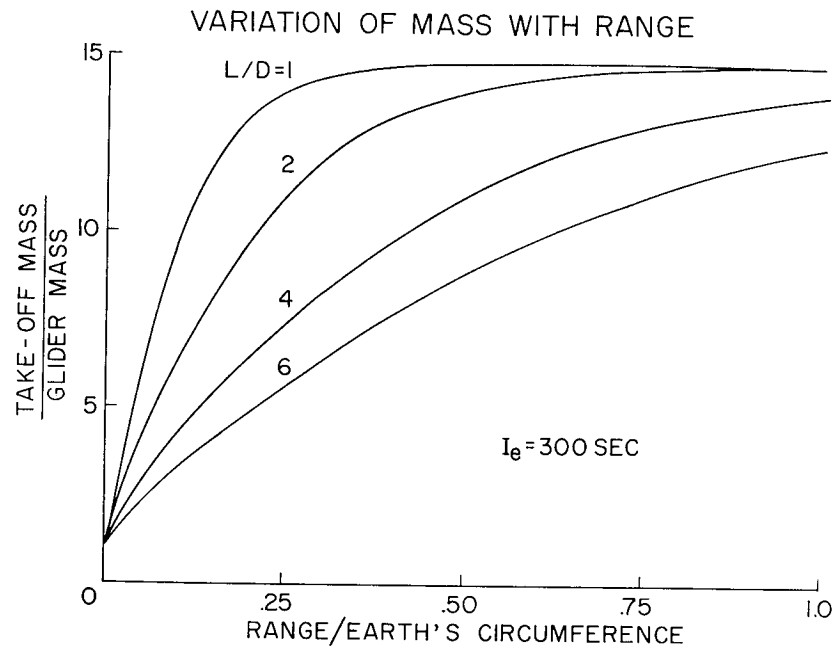


Figure 3.

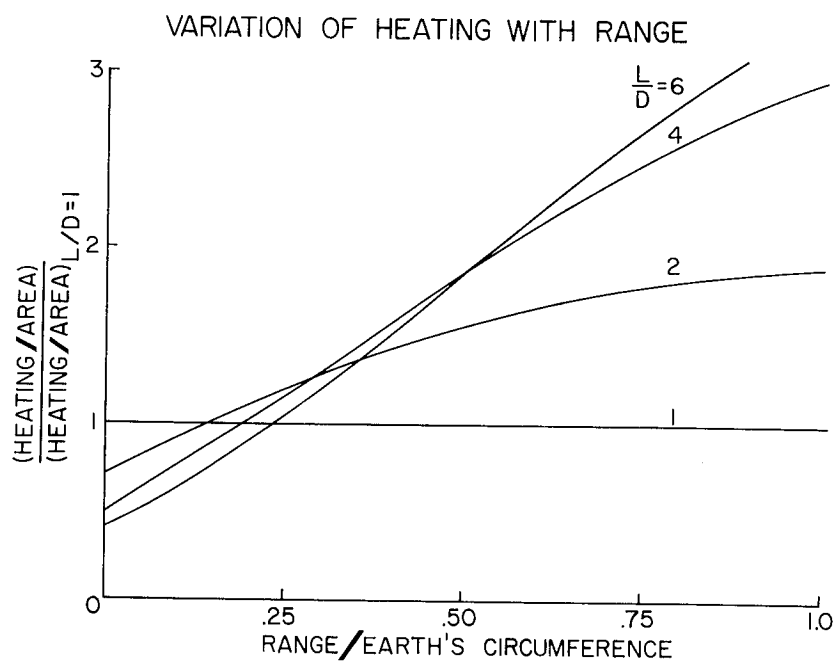


Figure 4.

## EVOLUTION OF FLAT-TOP WING-BODY COMBINATION

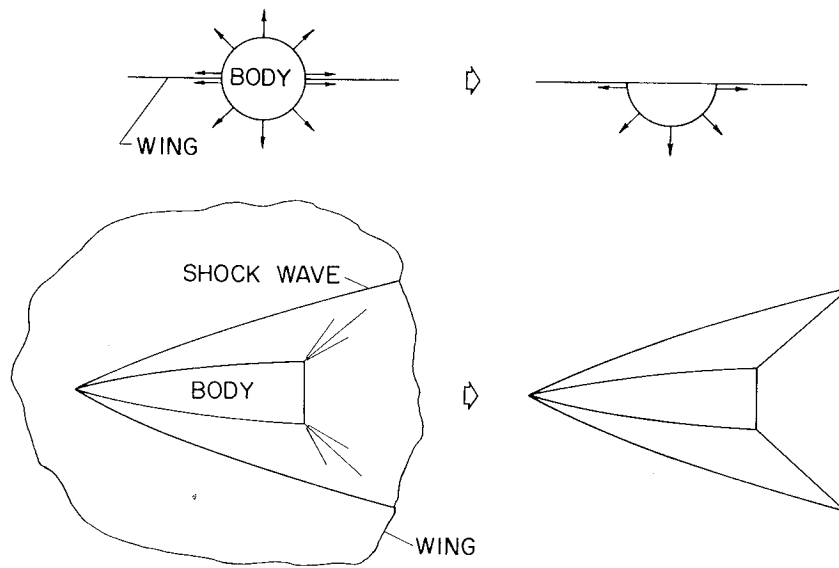


Figure 5.

## EVOLUTION OF FLAT-TOP AIRCRAFT CONFIGURATION

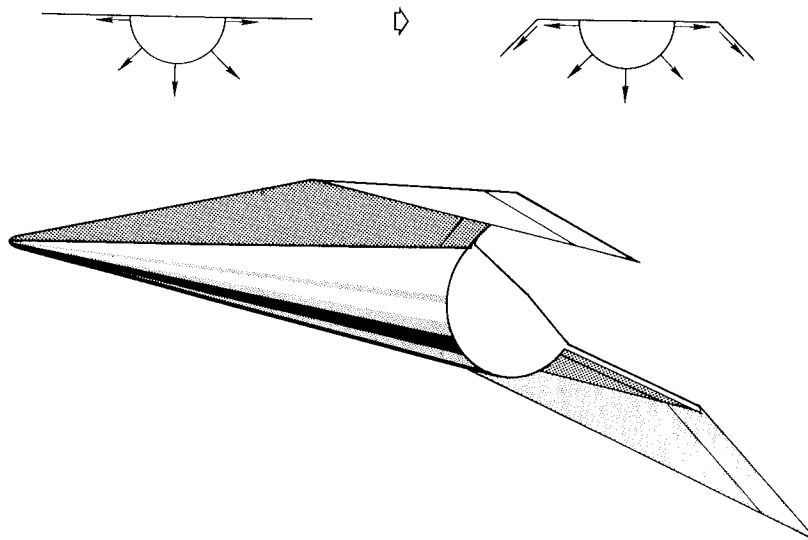


Figure 6.

# EQUATIONS FOR MAXIMUM LIFT-DRAG RATIO

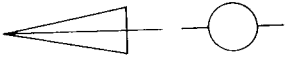

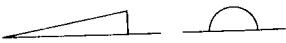
CONFIGURATION	$\left(\frac{L}{D}\right)_{MAX}$
	$\frac{C_{L\alpha}}{2\sqrt{C_{L\alpha}C_{D0}}} = \frac{1}{2}\sqrt{\frac{C_{L\alpha}}{C_{D0}}}$
	$\frac{C_{L\alpha}}{2\sqrt{C_{L\alpha}C_{D0}} -  C_L - C_{A\alpha} _0}$
	$\frac{C_{L\alpha}}{2\sqrt{C_{L\alpha}C_{D0}} +  C_L - C_{A\alpha} _0}$

Figure 7.

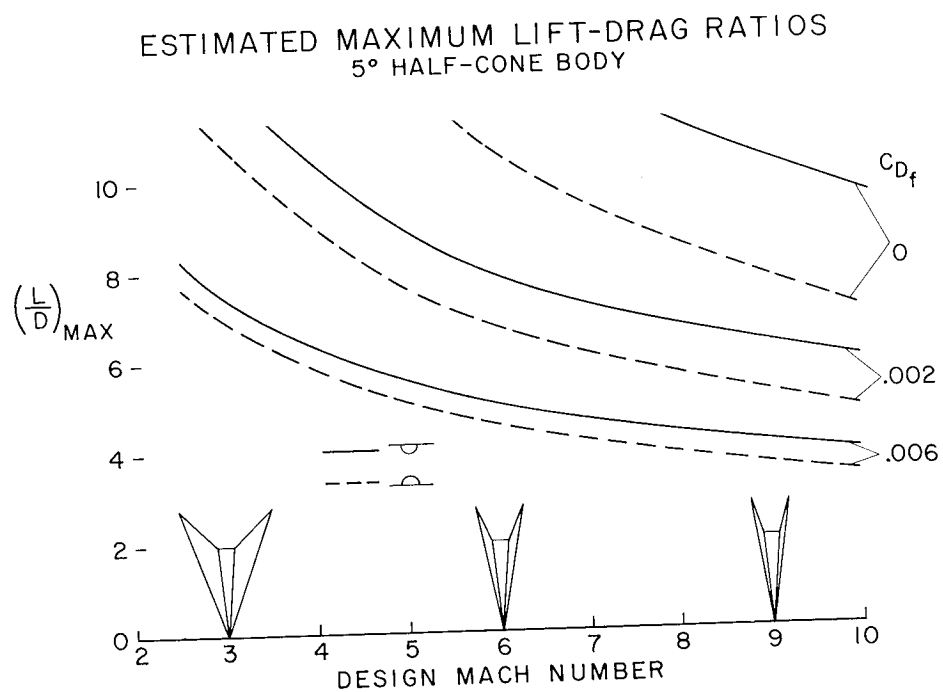


Figure 8.

# EFFECT OF CONE ANGLE ON MAXIMUM LIFT-DRAG RATIO

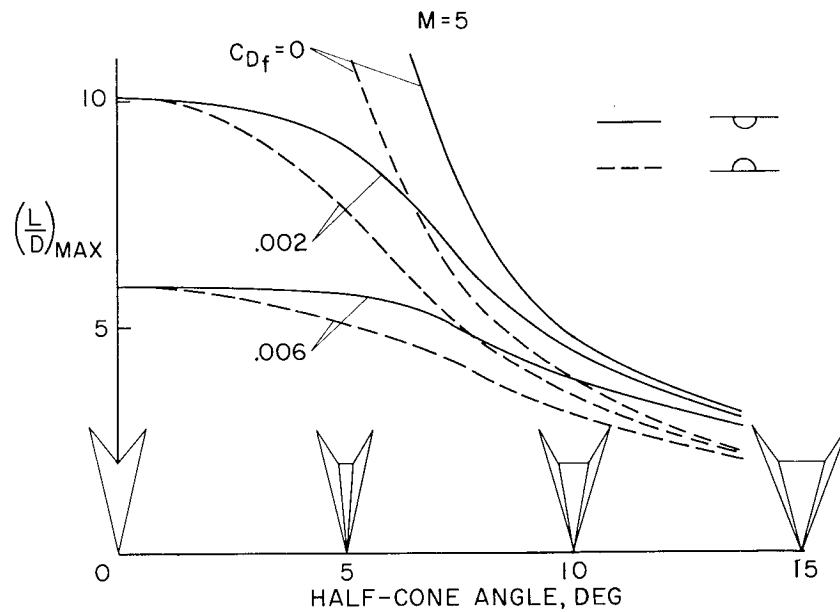


Figure 9.

## MEASURED MAXIMUM LIFT-DRAG RATIOS

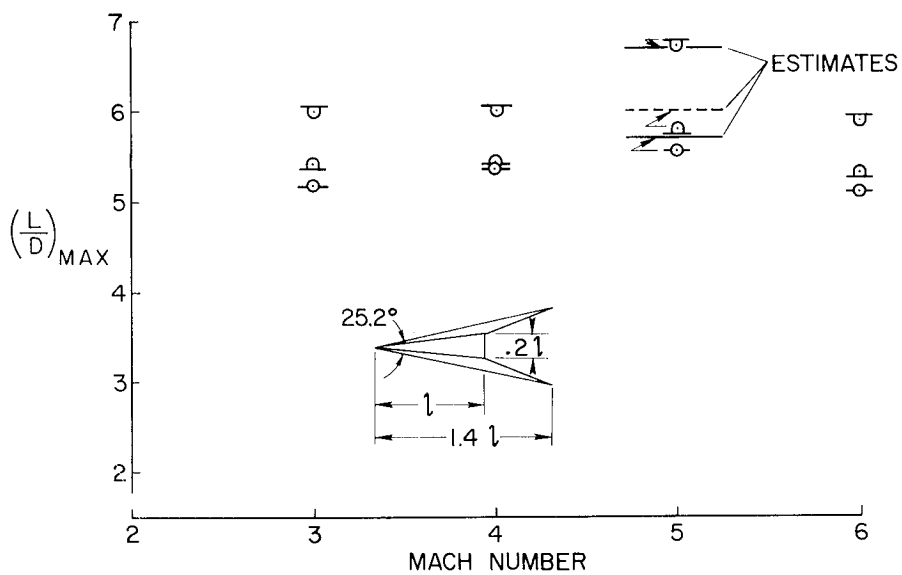


Figure 10.

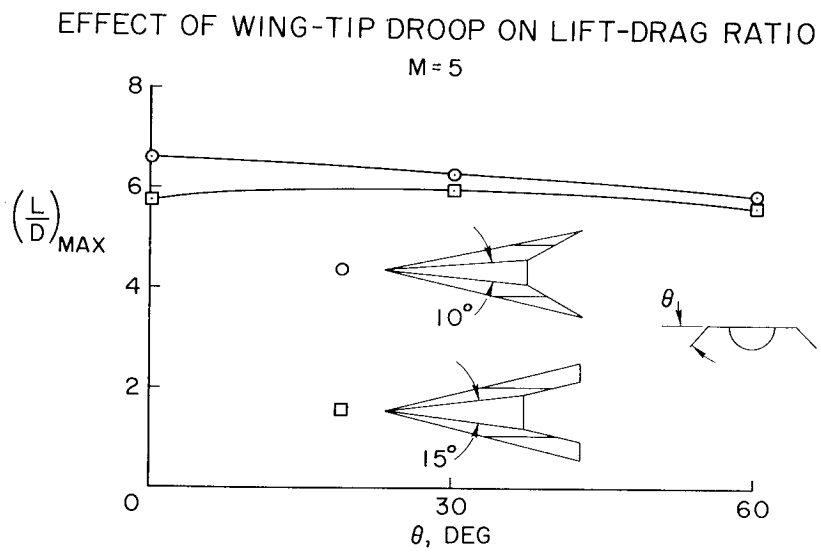


Figure 11.

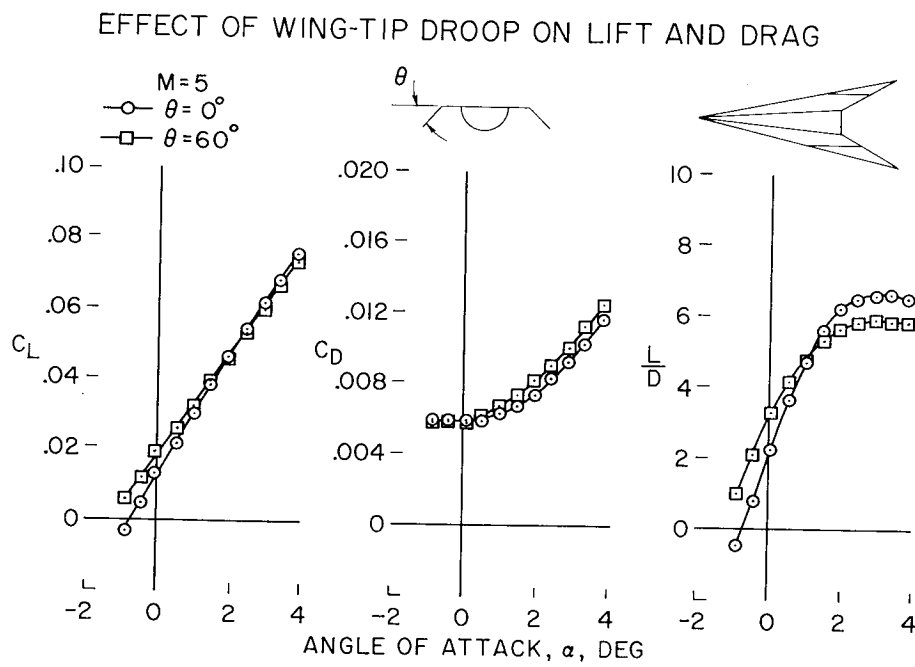


Figure 12.

# HYPERSONIC SIMILARITY RULE

$$\text{IF: } \left(M \frac{t}{c}\right)_1 = \left(M \frac{t}{c}\right)_2$$

$$\left(M \frac{b}{c}\right)_1 = \left(M \frac{b}{c}\right)_2$$

$$\left(M \alpha\right)_1 = \left(M \alpha\right)_2$$

$$\text{THEN: } \left(M^2 C_L\right)_1 = \left(M^2 C_L\right)_2$$

$$\left(M^3 C_{Dp}\right)_1 = \left(M^3 C_{Dp}\right)_2$$

$$\left(M^2 C_m\right)_1 = \left(M^2 C_m\right)_2$$

Figure 13.

## LIFT-DRAG RATIOS ACCORDING TO SIMILARITY RULE

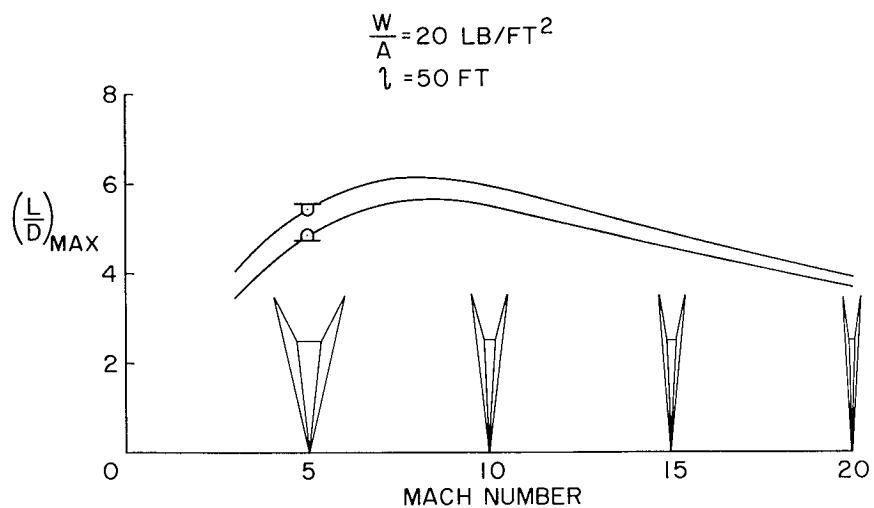


Figure 14.

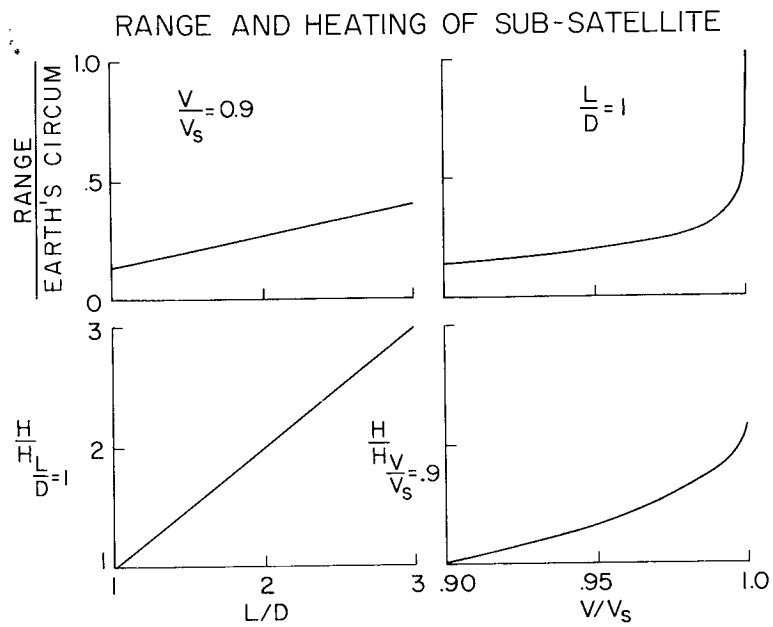


Figure 15.

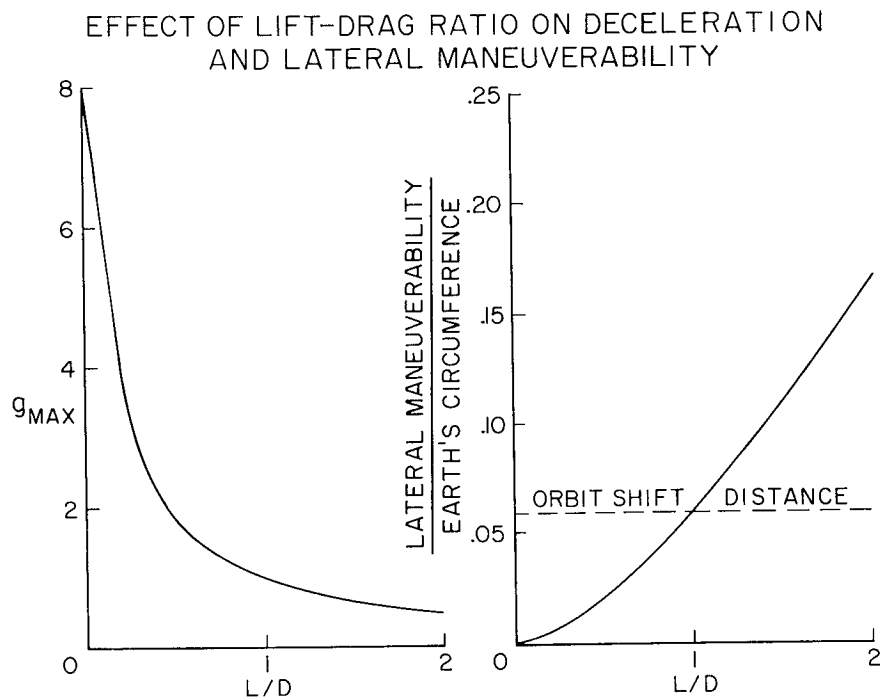


Figure 16.

# EFFECT OF BANK ON MOTION AND HEATING

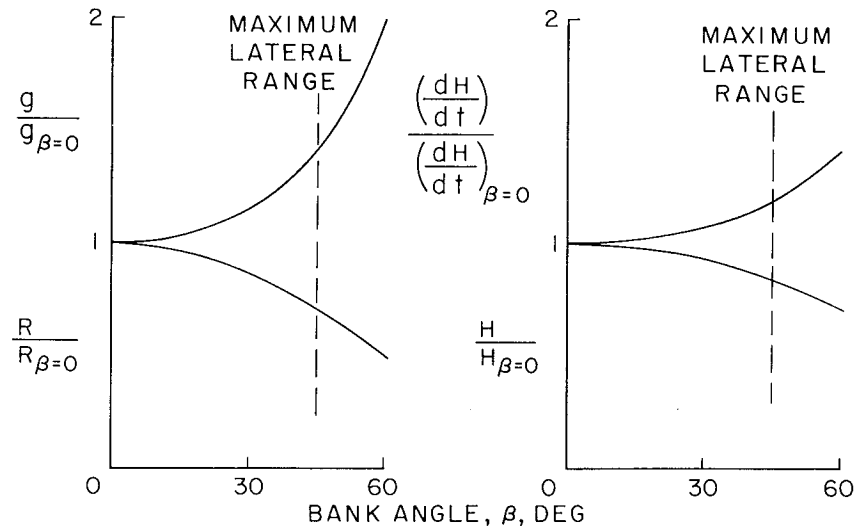


Figure 17.

# EVOLUTION OF FLAT-TOP BODY

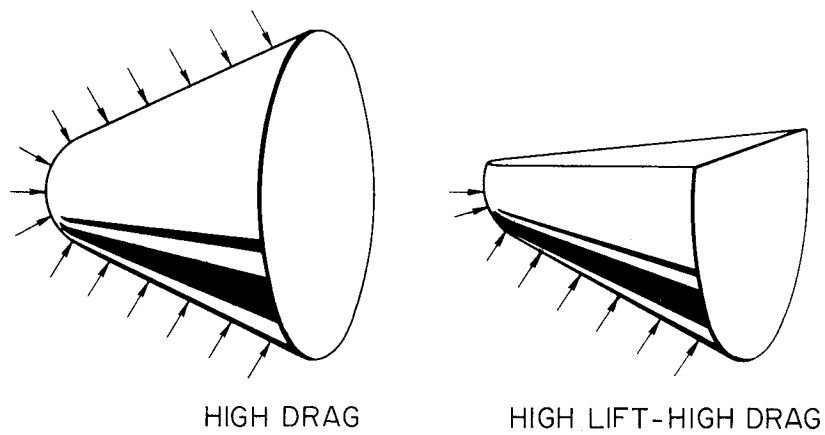


Figure 18.



# ESTIMATED LIFT AND DRAG OF HALF CONES

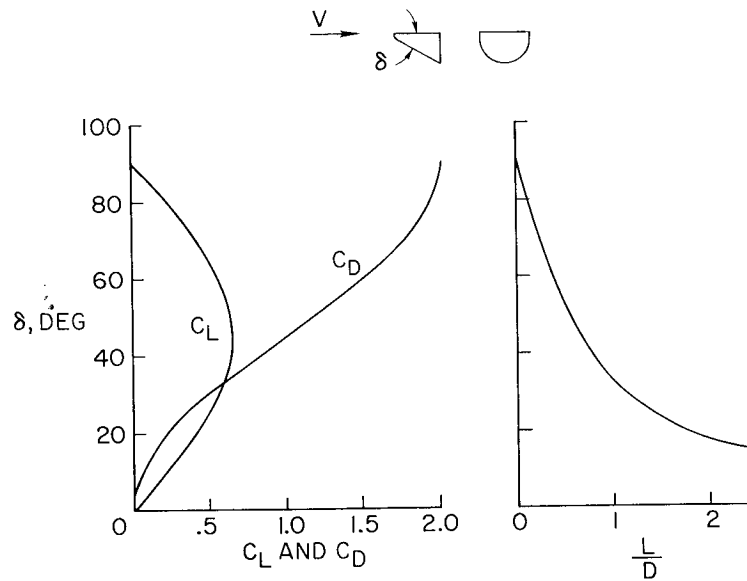


Figure 19.

# GENERALIZED HEATING OF HALF CONES

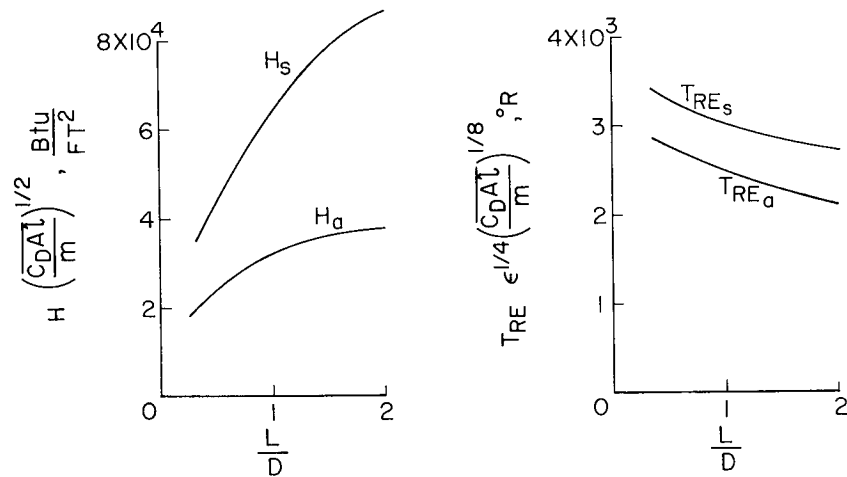


Figure 20.

# SUB-SATELLITE CONFIGURATION EMPLOYING A BLUNT HALF-BODY

A-23421

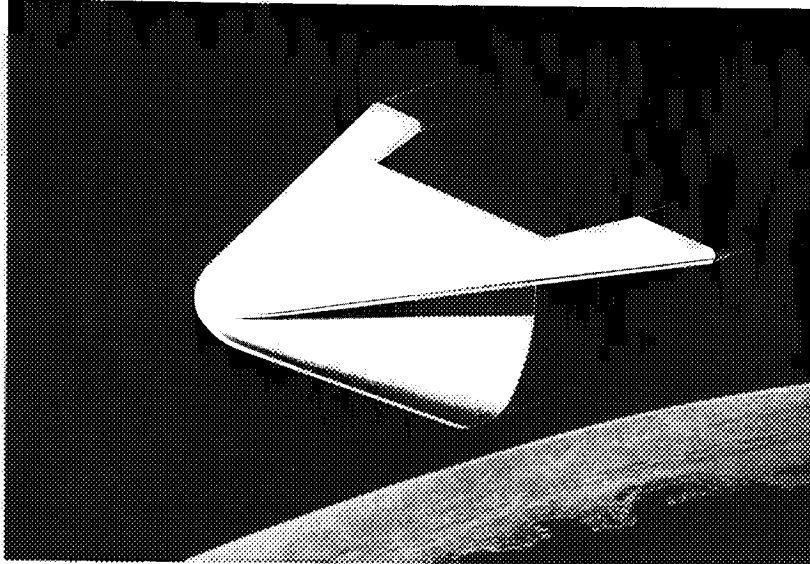


Figure 21.

## LONGITUDINAL CHARACTERISTICS OF BLUNT CONFIGURATION

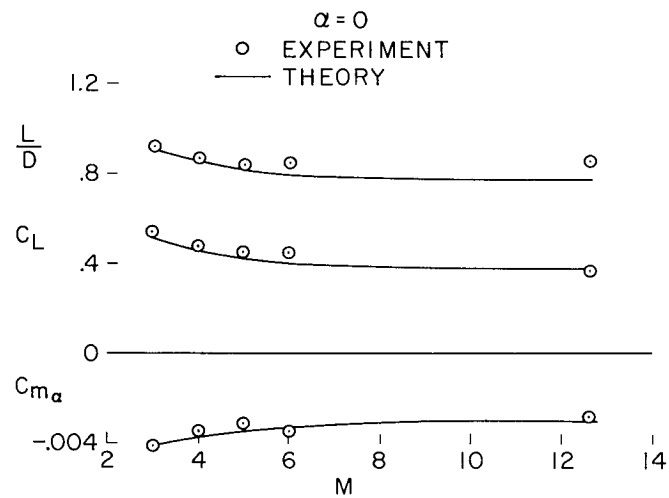


Figure 22.

A MORE SLENDER CONFIGURATION WITH  
CONVENTIONAL LANDING POTENTIAL

A-23621-29

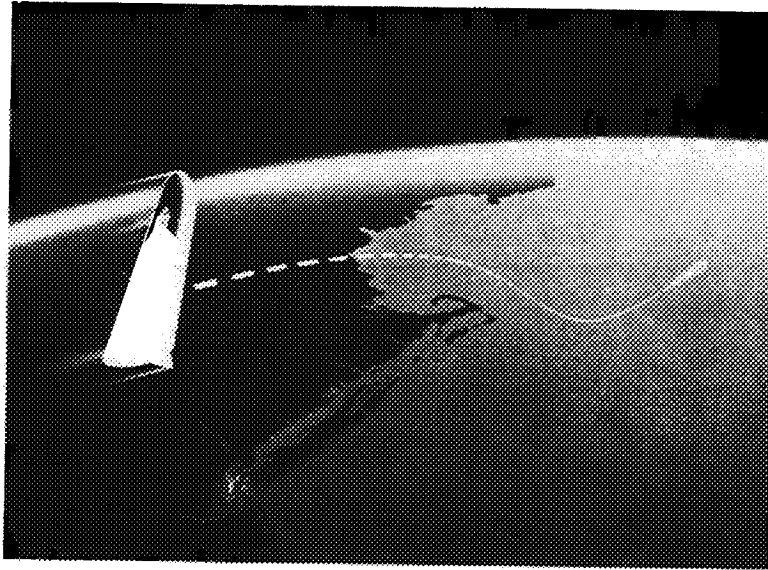


Figure 23.

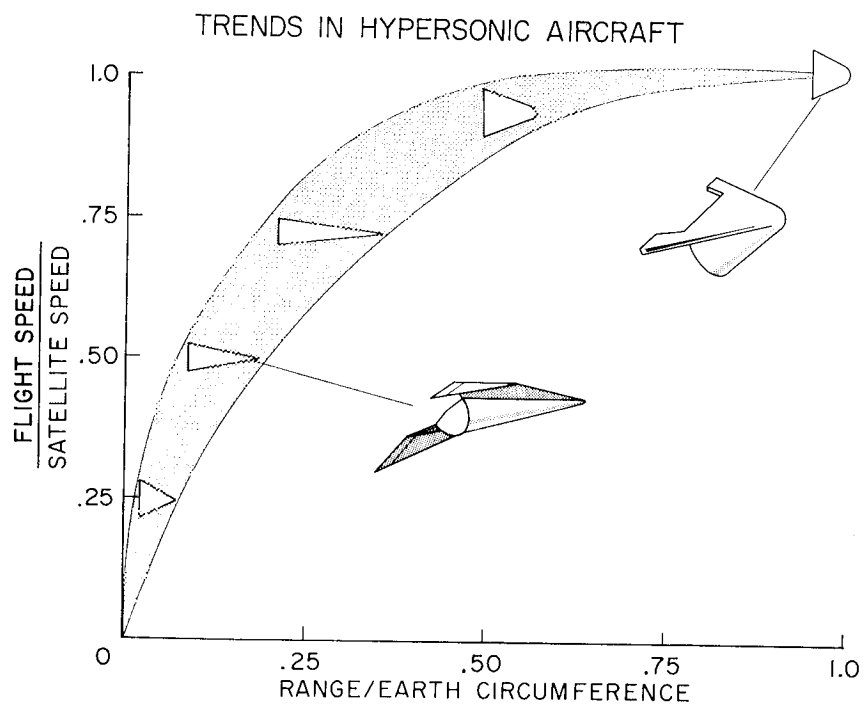


Figure 24.